Interaction between Strong Sound Waves and Cloud Droplets: Theoretical Analysis

YING-HUI JIA,[a] FANG-FANG LI,[a] KUN FANG,[b] GUANG-QIAN WANG,[b,c] AND JUN QIU[b,c]

[a] *College of Water Resources and Civil Engineering, China Agricultural University, Beijing, China*
[b] *State Key Laboratory of Hydroscience and Engineering, Tsinghua University, Beijing, China*
[c] *State Key Laboratory of Plateau Ecology and Agriculture, Qinghai University, Xining, China*

(Manuscript received 9 December 2020, in final form 10 August 2021)

ABSTRACT: Recently, strong sound wave was proposed to enhance precipitation. The theoretical basis of this proposal has not been effectively studied either experimentally or theoretically. On the basis of the microscopic parameters of atmospheric cloud physics, this paper solved the complex nonlinear differential equation to show the movement characteristics of cloud droplets under the action of sound waves. The motion process of an individual cloud droplet in a cloud layer in the acoustic field is discussed as well as the relative motion between two cloud droplets. The effects of different particle sizes and sound field characteristics on particle motion and collision are studied to analyze the dynamic effects of thunder-level sound waves on cloud droplets. The amplitude of velocity variation has positive correlation with sound pressure level (SPL) and negative correlation with the frequency of the surrounding sound field. Under the action of low-frequency sound waves with sufficient intensity, individual cloud droplets could be forced to oscillate significantly. A droplet smaller than 40 μm can be easily driven by sound waves of 50 Hz and 123.4 dB. The calculation of the collision process of two droplets reveals that the disorder of motion for polydisperse droplets is intensified, resulting in the broadening of the collision time range and spatial range. When the acoustic frequency is less than 100 Hz (at 123.4 dB) or the SPL is greater than 117.4 dB (at 50 Hz), the sound wave can affect the collision of cloud droplets significantly. This study provides a theoretical perspective of the acoustic effect on the microphysics of atmospheric clouds.

KEYWORDS: Atmosphere; Cloud droplets; Acoustic measurements/effects; Weather modification

1. Introduction

In recent years, sound waves have been widely applied in weather modification (Wei et al. 2021), particle agglomeration (Hoffmann 2000), and other fields. Acoustic agglomeration is a group effect of microparticle group systems under the action of sound waves (Zu et al. 2017). It realizes rapid agglomeration of particles. A study reveals that under the action of sound waves, the proportion of large-sized particles in aerosol increases, whereas the concentration of particles decreases (Hoffmann 2000). Zhang et al. (2020) observed apparent agglomeration after particle collision caused by surface cohesive force under the action of sound waves, by scanning electron microscopy. Gallego-Juárez et al. (1999) applied acoustic agglomeration technology to reduce coal-fire smog in factories. Numerical simulation of acoustic agglomeration using the population balance model (Sheng and Shen 2006) or the discrete element method–computational fluid dynamics (CFD-DEM; Kačianauskas et al. 2018) model has also been performed.

The mechanism of acoustic agglomeration is related to the complex dynamical effect of the particle phase and fluid phase under the action of sound waves. Many studies have attempted to explain this phenomenon. Hassan and Kawaji (2008) experimentally and theoretically discussed the influence of the frequency and viscosity of the oscillating fluid on the movement of small particles in it. Sujith et al. (1999) attempted to use the numerical integration and spectral analysis methods to study the relative motion between particles and between particles and fluid in sound field to explain the phenomenon of momentum and heat transfer in multiphase flow. Fan et al. (2013) simulated the variation in the collision time of two $PM_{2.5}$ particles of equal diameter, with particle size, distance, sound pressure level (SPL), and sound frequency. Zeng et al. (2020) explored the mobilization of a trapped nonwetting droplet by wall vibration, and he found that the droplet could pass through the throat when the amplitude of the excitation acceleration exceeds a critical value at a certain frequency. Dong et al. (2006) proposed the concept of effective agglomeration length, that is, the maximum distance at which particles can effectively collide. He calculated the effective aggregation length of two particles of different sizes under the action of sound waves of different frequencies and SPLs. Many studies (Amiri et al. 2016; Markauskas et al. 2015; Shaw and Tu 1979; Zheng et al. 2019; Li et al. 2020) have theoretically analyzed the mechanism of acoustic agglomeration and attempted to express it by mathematical formula. In general, the mechanisms of acoustic agglomeration include codirectional agglomeration, hydrodynamic effects, acoustic turbulence, and Brownian motion. The codirectional agglomeration mechanism refers to the collision caused by the relative motion between particles resulting from the difference in the carrying effects of sound waves across particles. The hydrodynamic effect mainly describes the collision caused by the deformation of the flow field as a result of the movement of the particles. Acoustic turbulence refers to the generation of turbulence in a flow field at a high SPL, resulting in collisions between particles under the action of inertia and diffusion. The Brownian motion describes the agglomeration caused by the irregular motion of submicrometer particles (Otto and Fissan 1999). These mechanisms have been extensively studied in the removal of

Corresponding author: Jun Qiu, aeroengine@tsinghua.edu.cn

DOI: 10.1175/JAMC-D-20-0278.1

hazardous particles from aerosols. To identify the mechanism of the action of sound waves, scholars have studied the forces on suspended particles in sound field. Knoop and Fritsching (2014) compared calculated acoustic force with van der Waals force as well as the interparticle adhesive force under liquid bridging. Sepehrirahnama et al. (2015) proposed a numerical method for calculating the acoustic wave force for multiple spheres in viscous fluids.

Most of the available studies consider soot aerosol particles of size 10 μm or less as the research objects. There are few studies on the acoustic agglomeration of cloud droplets of larger sizes. Clouds and precipitation are generated and evolve under certain weather conditions, which are related to most of the important weather phenomena.

Presently, the growth mechanism of cloud droplet is generally accepted to include the processes of condensation growth and collision growth (Wallace and Hobbs 2006; Sheng et al. 2003; Zhang et al. 2012). Condensation growth dominates the early stage of cloud droplet growth. Collision growth mainly includes the process wherein cloud droplets initially gather into large cloud droplets (capture water droplets), and rapidly falling large cloud droplets colliding with other small cloud droplets. Gravitational and turbulent coalescence of cloud droplets is thought to be the main process leading to rain formation (Akimov 2004). The cloud droplet is of an equal magnitude of size as a dust particle. The concept of using sound waves to intervene and promote the agglomeration of cloud droplets to enhance precipitation is an extension of the application of acoustic agglomeration. Grabowski and Wang's study (Grabowski and Wang 2013) established that turbulence can effectively promote the collision efficiency of cloud droplets in a cloud. The study by Amiri et al. (2016) demonstrated that turbulence occurs in a sound field when the SPL is above a threshold. Wei et al. (2020) discovered that wave-introduced turbulence could enhance the carrying and transport capacity of the flow. Mednikov and Larrick (1965) observed that turbulence caused by a sound field plays an important role in acoustic agglomeration. Tulaikova (2015) also described methods and devices for using sound waves to enhance precipitation in natural clouds. Meanwhile, acoustic agglomeration is also applied for fog dispersal (Liu et al. 2020). The experimental results of Zhang et al. (1963) and Hou et al. (2002) demonstrated that the existence of sound waves was beneficial for the disposal of water fog. While Hou et al. (2002) concluded that low frequency and high sound intensity was conducive to the dissipation of water mist. Experiments with artificial fog in a chamber had been conducted and a frequency in the range from 170 to 200 Hz turned out to be the most efficient (Galechyan 2005). Qiu's experiments show that the threshold SPL for the effective agglomeration of cloud droplets ranges from 114 to 121 dB when the sound frequency is 35–100 Hz (Qiu et al. 2021). The fog formed by the condensation of the water vapor in air is a type of cloud close to the ground surface. It can be inferred that sound waves can promote the agglomeration of cloud droplets. Under this assumption, this study calculates and studies the motion and collision process between cloud droplets under the action of sound waves.

In this study, the cloud droplets in a cloud layer are set as the research objects. Their physical behavior in a sound field is studied. Starting from an individual particle, the characteristics of cloud droplet motion caused by sound wave oscillation is revealed. Then, the collision time between two cloud droplets is calculated to explore the effect of sound waves on particle collision, considering the influence of particle size, acoustic frequency, and SPL. The research on the cloud droplets behavior in a sound field aids in better explaining the mechanism of acoustic precipitation enhancement and providing theoretical guidance for the practical application of acoustic precipitation.

2. Method

a. Description of sound wave

This study considers a traveling wave emitted from the ground to the cloud. The air velocity vibration caused by a similar traveling wave is illustrated by

$$u_f = u\sin(\omega t - kx), \tag{1}$$

where u_f is the flow rate at the position x in the sound field at the moment t (m s^{-1}), u is the velocity amplitude of the fluid driven by the sound wave (m s^{-1}), ω is the angular velocity of the sound field oscillation [rad s^{-1}; $\omega = 2\pi f$, where f is the vibration frequency (Hz)], k is the number of sound waves in the sound field [$k = 2\pi f/c$, where c is the velocity of sound waves in air (m s^{-1})], x is the position in the sound field (m), and t is time (s).

The SPL corresponding to each u can be obtained by (Talty 1998)

$$u = \sqrt{2I/(\rho_g c)}, \quad \text{and} \tag{2}$$

$$I = I_0 \times 10^{\mathrm{SPL}/10}, \tag{3}$$

where I indicates the intensity of the sound field strength (W m^{-2}), ρ_g is the density of air ($=1.293$ kg m^{-3}), I_0 is the standard reference value ($=10^{-12}$ W m^{-2}), and SPL is in decibels.

b. Force on droplet

A series of studies have been conducted to determine the force of spherical particles in a flow field, and a theoretical system has been developed (Kim et al. 1998; Mei et al. 1991). The unsteady motion of a rigid sphere particle in incompressible viscous fluid was studied by Basset (1888) and Oseen (1927). Mei and Adrian (1992) further discussed the unsteady drag exerted on a stationary sphere by oscillation flow at finite Reynolds number. Cleckler et al. (2012) numerically solved the motion of heavy spherical particles in a sound field and verified their results with experiments. They also studied the applicable range of the linearized Stokes equations. According to Maxey and Riley (1983), the force on the particles in a fluid mainly includes the following five components.

1) Viscous drag

Viscous drag acts on particles when there is a relative motion between the particles and fluid:

$$F_1 = C_D \frac{\rho_g |u_f - v|(u_f - v)}{2} \frac{\pi d^2}{4}, \quad (4)$$

where F_1 is the viscous drag (N), v is the velocity of droplets (m s^{-1}), d is the particle diameter (m), and C_D is the drag coefficient; C_D is related to the Reynolds number $\mathrm{Re}_d = \rho_g d|u_f - v|/\mu$, where μ is the dynamic viscosity of air (17.9×10^{-6} Pa s). Because the Reynolds number is less than 20 in the calculation, C_D is calculated by (Seinfeld and Pandis 1998)

$$C_D = 24/\mathrm{Re}_d. \quad (5)$$

When $C_D = 24/\mathrm{Re}_d$, the viscous drag can be simplified to $F_D = 3\pi d\mu(u_f - v)$.

2) BASSETT FORCE

Basset force is also called unsteady viscous drag (a historical integral term). It indicates the increased resistance on a particle during the variable motion in a flow field and reflects the influence of the historical motion process. The Bassett force can be calculated by

$$F_2 = \frac{3}{2}\pi d^2 \mu \int_0^t \frac{\frac{d}{ds}(u_f - v)}{\sqrt{\pi v(t-s)}} ds, \quad (6)$$

where F_2 is the Bassett force on the particle (N) and v is the motion viscosity ($=\mu/\rho_g$).

3) ADDITIONAL MASS FORCE

Accelerated particles drive the surrounding fluids for combined accelerated motion. The force pushing the surrounding fluid to accelerate is called additional mass force, that is, virtual mass force. The additional mass force and the force acting on a sphere are a pair of interaction forces that can be calculated by

$$F_3 = -\frac{1}{2}\rho_g V \frac{d(u_f - v)}{dt}, \quad (7)$$

where F_3 is the additional mass force acting on the particle (N) and V is the volume of the particle.

4) PRESSURE GRADIENT FORCE

In a flow with a pressure gradient, a resultant force of pressure acts on the particle. The pressure gradient force acting on the sphere can be calculated by

$$F_4 = \rho_g V \frac{Du_f}{Dt}, \quad (8)$$

where F_4 is the pressure gradient force acting on the particle (N) and Du_f/Dt is the full differential of the velocity field u_f versus t.

5) GRAVITY AND BUOYANCY

Gravity is the force that acts on an object owing to the attraction of Earth. Because cloud droplets are always present in the atmosphere and are carried by the fluid, buoyancy acts on the particles. The F_5 in the following equation indicates the net gravity after subtracting the buoyancy:

$$F_5 = (\rho_p - \rho_g)Vg, \quad (9)$$

where g is the gravitational acceleration ($=9.81$ m s^{-2}) and ρ_p is the density of the cloud droplets ($=1000$ kg m^{-3}).

c. Numerical solution

The Lagrangian description format is adopted for the motion of cloud droplets. It tracks the motion path of the particles. The downward motion of cloud droplets under the action of gravity is calculated with the assumption that the particle motion does not affect the sound field around the spherical particles. Combining the forces on an individual particle in the flow field, the following equation can be established according to Newton's second law (Maxey and Riley 1983):

$$m_p \frac{dv}{dt} = C_D \frac{\rho_g |u_f - v|(u_f - v)}{2} \frac{\pi d^2}{4} + \frac{3}{2}\pi d^2 \mu \int_0^t \frac{\frac{d}{ds}(u_f - v)}{\sqrt{\pi v(t-s)}} ds + \frac{1}{2}\rho_g V \frac{d(u_f - v)}{dt} + \frac{\pi d^3}{6}(\rho_p - \rho_g)g + \rho_g V \frac{Du_f}{Dt}, \quad (10)$$

where m_p is the mass of the particle ($=\rho_p V$). The differential Eq. (10) is nonlinear, and the fourth-order Runge–Kutta method is used to numerically calculate the motion process of the cloud droplet. To calculate the value of the second historical integral on the right side of the equation, we discretized it and assumed that the acceleration within each time step is constant [i.e., $d(u_f - v)/ds$ = constant], so that the Bassett force at the current time can be obtained. The variation in the velocity and displacement with time is obtained from the results of the numerical solution. Meanwhile, the magnitude of each force can be calculated.

d. Cloud microphysical parameters

There are significant uncertainties in the microphysical properties of cloud layers. The particle size of cloud droplets exhibits wide variation and is mainly concentrated around 1–20 μm (Wieprecht et al. 2005). Atmospheric cloud physics considers the typical particle size of cloud droplets to be 10 μm, cloud droplets of 50 μm to be large droplets, and the boundary line between cloud droplets and raindrops to be 100 μm (Sheng et al. 2003). Because this study mainly analyses collision, and the growth of small cloud droplets depends mainly on condensation, the particle size of cloud droplets considered in this study is between 5 and 50 μm. The initial velocity in a stationary cloud layer is set to be zero. Observations of the properties of thunder sound under natural conditions reveal the peak sound frequency of thunder to be concentrated in the low-frequency range (Bhartend 1969; Bodhika et al. 2018; Yuhua and Ping 2012). Therefore, the frequency range of sound wave is set to be 20–500 Hz. As the SPL increases, the energy consumption and technical challenges associated with producing artificial sound waves increase. Liu et al. (2009) recommends that the SPL for acoustic agglomeration should not exceed 150 dB. Therefore, in this research, the SPL is set within the 60–150 dB range. The vertically downward direction is positive.

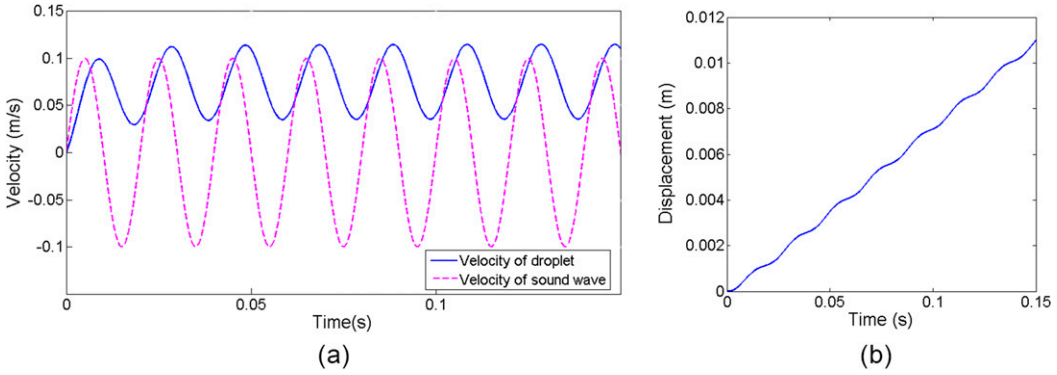

FIG. 1. Variation in (a) velocity of droplet and fluid with time and (b) droplet displacement, under the action of a sound wave with $f = 50$ Hz and SPL = 123.4 dB for a droplet with $d = 50\,\mu$m.

In the framework of this paper, the role of Brownian motion has been neglected. Brownian motion is known to be unpredictable, but there are some statistical laws. According to Newton's classical diffusion equation, the particle diffusion length can be calculated as follows:

$$\lambda = \sqrt{(x^2)} = \sqrt{2Dt}, \tag{11}$$

where x is the displacement of the particle, D is the diffusion coefficient, and t is time. The D can be calculated by the following formula:

$$D = \frac{kTC}{3\pi\mu d_P}, \tag{12}$$

where k is Boltzmann constant ($=1.38 \times 10^{-23}$ J K^{-1}), μ refers to the dynamic viscosity of the air, d_P is the particle size, and T is the absolute temperature (K). For larger particles, the slip correction coefficient C can be ignored. Assuming that $T = 273$ K, $\mu = 17.11 \times 10^{-6}$ Pa s, and a particle size of 10 μm, we can obtain $D = 2.336 \times 10^{-12}$ m^2 s^{-1}. The diffusion length range is [2.16, 6.84] μm, given a time t from 1 to 10 s (much larger than the range calculated in this article). This is much less than the displacement due to gravity-induced subsidence and acoustic stress. So, the effect of Brownian motion is not considered in the calculation case in this paper.

3. Impact of sound wave on individual cloud droplet

a. *Motion of individual cloud droplet in traveling wave field*

Under the action of sound waves, the velocity of an individual cloud droplet first experiences an unstable start-up period and then attains a relatively balanced oscillation state, as shown in Fig. 1a. The velocity at the center position of the oscillation in the latter state is named "equilibrium velocity." Herein, the oscillation frequency is consistent with that of the sound wave, whereas the oscillation amplitude is related to the properties of the sound wave and cloud droplet. Under the action of inertia and viscosity, a phase difference appears between the velocity of the cloud droplet and that of the fluid in the sound field. The velocity oscillation causes the displacement of the cloud droplets to fluctuate as shown in Fig. 1b. When the amplitude of the velocity oscillation is smaller than the equilibrium velocity, the fluctuation in the displacement is negligible. In all the cases, the equilibrium velocity of the cloud droplets is always higher than zero. This implies that cloud droplets generally move downward when there is no updraft.

Because the velocity of a cloud droplet eventually attains a stable oscillation, it can be expressed by

$$v = v_{\text{center}} + v_{\text{amplitude}}\Delta f(x,t), \tag{13}$$

where v_{center} represents the equilibrium velocity (mean velocity), $v_{\text{amplitude}}$ is the oscillation amplitude of the cloud drop velocity, and $f(x, t)$ is a function of time and position.

A droplet in still air settles under gravity and rapidly attains a constant velocity called the free settling velocity v_t (Finlay 2001). Under stable cloud conditions, air can be assumed to be stationary, that is, $u_f = 0$. The v_t for droplets of different sizes is calculated. The results reveal that the equilibrium velocity of droplet v_{center} does not vary with variation in the frequency and SPL of sound waves. Rather, it is equal to the free settling velocity v_t.

b. *Sound frequency effect on the motion of individual droplet*

Figure 2 shows the relationship between the velocity and displacement of a droplet of size 10 μm versus the sound frequency when the SPL of the sound wave is 123.4 dB. It is evident that the velocity of the droplet fluctuates around 0.003 m s^{-1} for all sound frequencies. Moreover, the amplitude of variation in the velocity decreases as the sound frequency increases. Under the action of sound waves of frequency 20 Hz, the velocity amplitude of cloud droplet oscillation approaches 0.1 m s^{-1}. This is almost equal to the velocity amplitude of the sound field. When the sound frequency increases from 200 to 500 Hz, the velocity amplitude of cloud droplet movement tends to decrease monotonously with a drop of 23%. The sound frequency does not impact the equilibrium velocity. However, the oscillation frequency of the cloud droplet velocity is consistent with the frequency of the sound wave.

c. *SPL effect on the motion of individual droplet*

Figure 3a shows the variation in the droplet displacement and velocity with the SPL of a sound wave of frequency 50 Hz

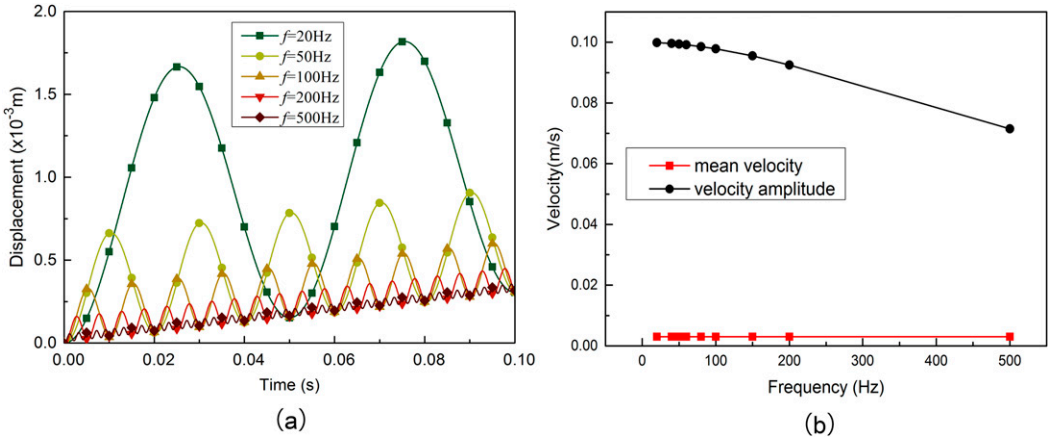

FIG. 2. Variation in (a) droplet displacement with time for different sound frequencies and (b) equilibrium velocity and velocity amplitude of droplet with sound frequencies, under the action of a sound wave with SPL = 123.4 dB ($u = 0.1\,\mathrm{m\,s^{-1}}$) for a droplet with $d = 50\,\mu$m.

for a droplet of 10 μm. Meanwhile, Fig. 3b shows the case for a droplet of 100 μm. It is evident that for a smaller droplet, the movement of droplet varies significantly with an increase in the SPL. Furthermore, the back and forth oscillation process caused by sound waves dominates the motion of small cloud droplets, whereas the displacement fluctuation caused by sound waves is not apparent for larger droplets.

A similar phenomenon is related to the magnitude relationship between the velocity amplitude and equilibrium velocity (Fig. 4). With the increase in the SPL, the velocity amplitude of the cloud droplet shows a rapid increasing trend. For a cloud droplet of 10 μm, a sound wave with a smaller SPL can produce a velocity oscillation that is significantly larger than the equilibrium velocity. Meanwhile, for a droplet of 100 μm, the droplet velocity amplitude does not attain its equilibrium speed even if the SPL attains 147 dB.

Figure 4 also indicates that the velocity of a droplet exhibits almost a linear relationship with the velocity amplitude of the sound field. The entrainment coefficients (Sujith et al. 1997) of the flow field vary for cloud droplets of different sizes. The slopes of the velocity amplitude in Fig. 4 are also different. The slope is approximately equal to one for a droplet of 10 μm, that is, the velocity amplitude of the cloud droplet is close to that of the fluid. For cloud droplets of 100 μm, the slope is significantly smaller than 1, as shown in Fig. 4d. Figures 3 and 4 also verify that the velocity of a cloud droplet fluctuates more significantly under the action of sound waves of larger SPL.

d. *Droplet size effect on the motion of individual droplet*

Figure 4 indicates that the equilibrium velocity does not vary with the SPL for cloud droplets of 10 and 100 μm. For a droplet of 10 μm, the equilibrium velocity remains at $0.003\,\mathrm{m\,s^{-1}}$. Meanwhile, for a droplet of 100 μm, the equilibrium velocity remains at $0.3024\,\mathrm{m\,s^{-1}}$, which is larger than the amplitude of the velocity, that is., the equilibrium velocity increases by two orders of magnitude when the droplet size increases by an order of magnitude. For a smaller droplet, a sound wave with a marginal SPL can produce a large oscillation,

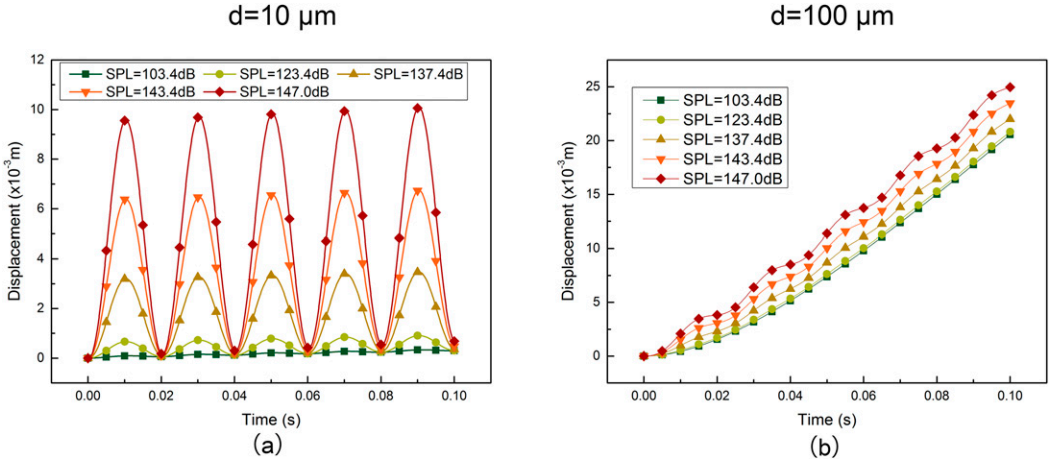

FIG. 3. Variation in droplet displacement with time under the action of sound waves of 50 Hz and different SPLs for droplet size d = (a) 10 and (b) 100 μm.

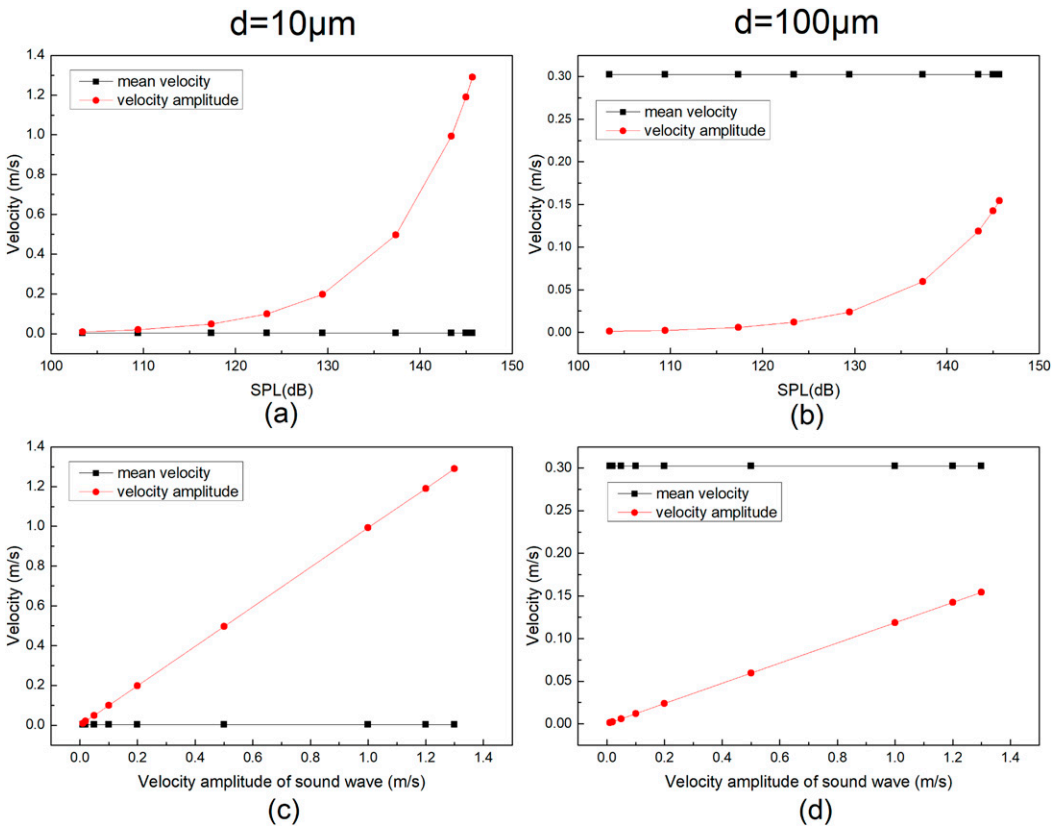

FIG. 4. Variation in droplet velocity under the action of sound waves of 50 Hz (a) with different SPLs for droplet size $d = 10\,\mu$m, (b) with different SPLs for droplet size $d = 100\,\mu$m, (c) with different velocity amplitudes for droplet size $d = 10\,\mu$m, and (d) with different velocity amplitudes for droplet size $d = 100\,\mu$m.

as indicated in Fig. 3a. For a larger droplet, the free settling velocity is high. Therefore, sound waves of higher SPLs are required to provide sufficient entrainment force to cause an apparent fluctuation.

Figure 5 shows the relationship of the cloud droplet displacement and velocity versus the droplet size under the action of sound waves of 50 Hz and 123.4 dB. As the droplet becomes larger, the equilibrium velocity also increases, resulting in different moving characteristics. When the droplet size is relatively small, the fluctuation amplitude of the droplet velocity is close to the velocity amplitude of the flow field (0.1 m s^{-1}). With an increase in the cloud droplet size, the equilibrium

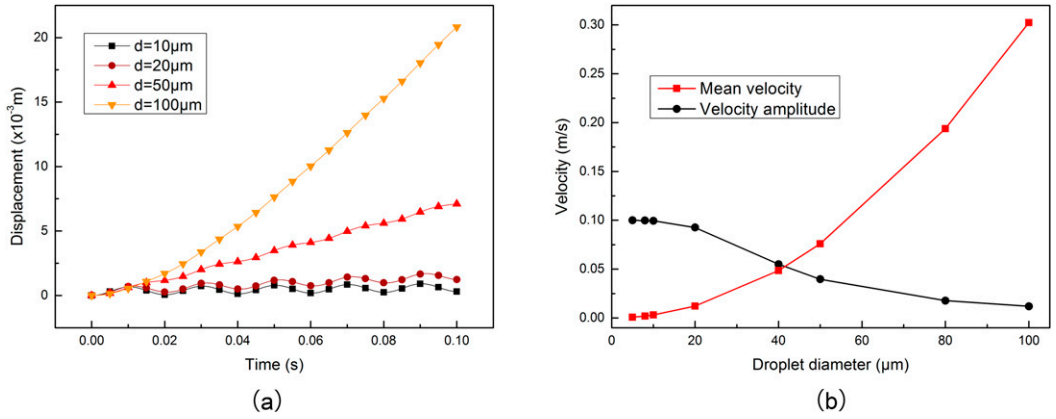

FIG. 5. Variation in (a) droplet displacement with time and (b) variation in equilibrium velocity and velocity amplitude with droplet size, under the action of sound waves of 50 Hz and 123.4 dB ($u = 0.1$ m s^{-1}).

TABLE 1. Distance of two equal-sized cloud droplets after 2-s motion under the action of sound waves with an initial distance of 1000 μm. It is assumed that the droplet diameter at a higher position of the sound field is d2. The position of its center is set as the original point. The droplet diameter at the lower position of the sound field is d1, and its center is located at $x = 1$ mm.

Droplet size d1 = d2 (μm)	5	10	20	50	80	90	100
Distance at $t = 2$s (μm)	1000.107	1000.227	1000.496	1001.096	1001.622	1001.805	1001.988

velocity of the droplet under the action of gravity becomes significantly higher than that of the flow field, such that the oscillation of the displacement is no longer significant.

In this study, the cloud droplet is considered to be sensitive to sound wave action when the velocity amplitude of droplet oscillation driven by sound wave equals to its maximal free settling velocity, which is also the equilibrium velocity.

Figure 5b indicates that the equilibrium velocity is comparable to the velocity amplitude caused by a sound wave for a cloud droplet of 40 μm. With the increase in the droplet size, the displacement increases, and the oscillation of the displacement weakens. For a droplet of 100 μm, the displacement variation with time forms an almost straight line without fluctuation, as shown in Fig. 5a. Therefore, at constant acoustic energy, the change of moving characteristics and the oscillation of velocity are the two main aspects of the influence of sound waves on the droplet. Meanwhile, the effect of the acoustic wave with same energy on the motion of large-sized droplets is relatively weak. It can be concluded from Fig. 5 that there exists a size threshold of the droplet being easily driven by sound waves of 50 Hz and 123.4 dB, which is equal to 40 μm, that is, those droplet smaller than 40 μm can be easily driven by this sound, while those larger than 40 μm can be hardly driven by the same sound.

4. Impact of sound wave on collision of two cloud droplets

a. Collision occurrence condition

Traditional atmospheric cloud physics (Sheng et al. 2003; McDonald 1958) considers the typical number density of cloud droplets to be $10^9\,\mathrm{m}^{-3}$. With the assumption of $10^9\,\mathrm{m}^{-3}$ and that the cloud droplets in a cloud layer are distributed uniformly, the average spacing between two cloud droplets is calculated to be 1000 μm (i.e., 1 mm). Hence, in this study, the given distance between two cloud droplets is set to be 1 mm.

To verify the likelihood of collision of two equal-sized cloud droplets separated by 1 mm under the action of gravity field and sound field without initial velocity, their distance after 2 s motion under the action of sound waves of 50 Hz and 123.4 dB is calculated, as presented in Table 1. After 2 s, the two droplets are still at a considerable distance (approximately 1000 μm), and the variation in the distance is from a few tenths of micrometers to several micrometers and tends to increase. This demonstrates that under the action of traveling waves, cloud droplets of equal size and different initial positions are unlikely to collide while falling simultaneously.

The solution of an individual droplet indicates that the average falling velocity of droplets of larger size is higher. Thus, it can be inferred that two cloud droplets without initial velocity can collide only when the droplet in the upper sound field is larger than that in the lower part. It should be noted that the assumption of zero initial velocity might seem to be idealistic, but it is reasonable and does not affect the validity of results because the initial relative velocity will only lead to the constant offset of the collision time of the two droplets.

b. Sound frequency effect on the collision of two droplets

The coefficient of the collision time under the action of sound waves is defined to describe the time variability of two cloud droplet collisions, as illustrated by

$$\eta_t = \frac{t - t_0}{t_0}, \tag{14}$$

where t is the collision time of droplets under the action of sound waves and t_0 is the collision time of droplets without considering sound waves. The positive value of η_t indicates that the time required for collision is prolonged under the action of sound waves. The negative value indicates that the time is shortened. Figure 6 shows the variation in the collision time of two cloud droplets with sound frequency for different droplet combinations. Figure 6 shows that the collision time of two cloud droplets presents a complex and variable relationship with the sound frequency. This is mainly a result of the variations in both the displacement magnitude and the phase position change of the droplets caused by the variation in the sound frequency. When the sound frequency is below 100 Hz, the collision time exhibits a significant fluctuation and an unstable state with the variation in frequency. Its range is presented in Table 2. The collision time variation range for droplets with different size combinations is from −10.8% to 49.1% for a sound of 20 Hz, from −16.5% to 12.1% for a sound of 50 Hz, from −12.9% to 15.1% for a sound of 80 Hz, and from −9.13% to 6.92% for a sound of 100 Hz.

The coefficient of the collision location under the action of sound waves is defined to describe the spatial variability of two cloud droplet collisions, as illustrated by

$$\eta_s = \frac{s - s_0}{s_0}, \tag{15}$$

where s is the collision location of droplets under the action of sound waves and s_0 is the collision location of droplets without considering sound waves. Figure 6 shows that the coefficient of the collision location is always positive; that is, the displacement is larger than that without sound wave action. Coefficient η_s tends to be zero as the sound frequency increases. Meanwhile, with the increase in d1, the variation in the collision time and location reduces. The maximal η_s under different sound frequencies (presented in Table 2) indicates that the increment in the displacement generally decreases

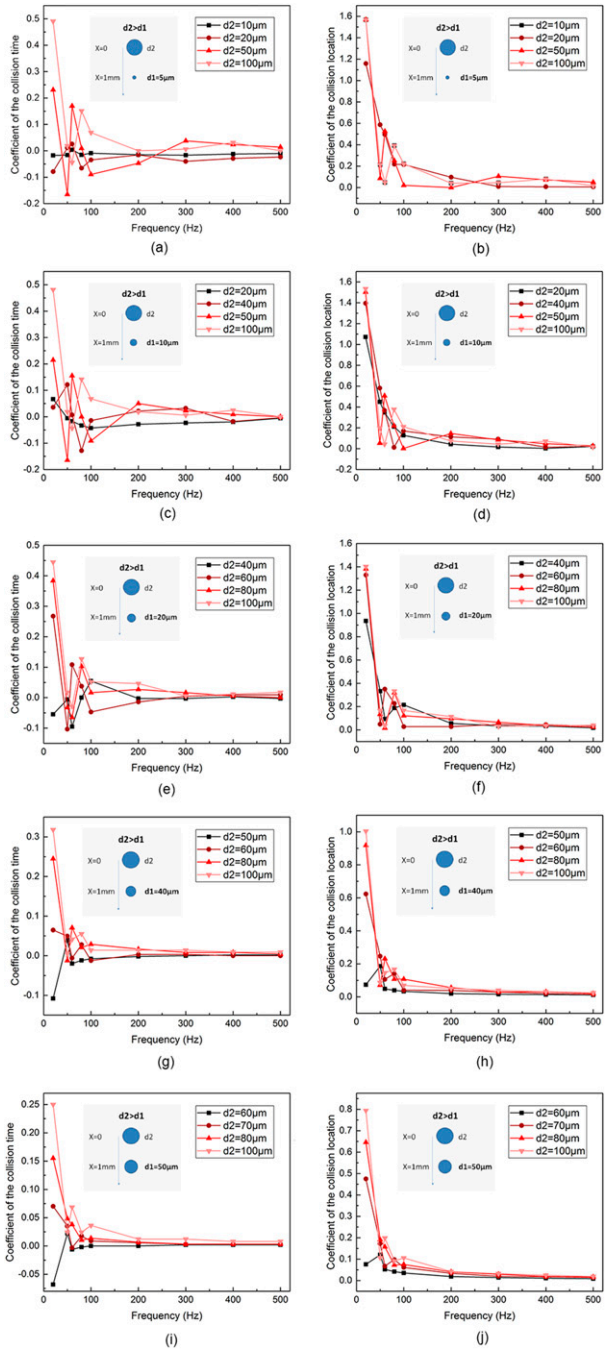

FIG. 6. Variation in coefficient of collision (left) time and (right) location with sound frequency for different droplet size combinations, under the action of sound waves of 123.4 dB.

with increasing frequency. It can be concluded that under the action of sound waves, the collision–coalescence process of polydisperse cloud droplets is elongated on both spatial and temporal scales. This means that in certain conditions, polydisperse cloud droplets collide in a larger space, which could be related to enhanced precipitation, but further study is in need.

Figure 7 shows the positional variations for a droplet combination of d1 = 5 and d2 = 50 μm at the sound frequencies of 20, 50, 60, and 100 Hz. The red and blue lines indicate the locations of droplets d1 and d2 with and without sound waves, respectively. For the frequencies of 20 and 60 Hz, the blue lines exhibit apparent fluctuation and intersect near the peak of the displacement curve of d1. The intersection points of the two blue lines appear after the intersection of the red lines, that is, the collision time is extended, and the displacement to the collision location increases. For the frequencies of 50 and 100 Hz, the two blue curves intersect near the trough of the displacement curve of d1, and the collision time is relatively advanced. The variation in the motion period and the amplitude of the displacement fluctuation caused by the variation in the sound frequency results in the irregular variation in the collision time and location. Therefore, the collision may occur at any phase.

A subdivision of the frequency gradient for lower frequencies may result in further complex fluctuations in the collision time, as well as more extremes. It is evident that with the increase in the sound frequency, the curves under the action of sound waves gradually approach those without sound waves, that is, the collision time and location come close to the case of no sound waves. In general, for cloud droplets of different size combinations, both the cases (one where sound waves increase the collision time and the other where they reduce it) exist. Moreover, for the case of relative high frequency, the effect of sound waves on collision between droplets becomes unapparent. For the case wherein the collision time is prolonged significantly, the displacement to the collision location also increases significantly.

The results reveal that the entrainment effect of a sound wave of lower frequency is stronger for an individual cloud droplet, and the motion of the droplet is more intense. Meanwhile, for two or more droplets, the collision efficiency is closely related to the property of the droplets, and its variation with the sound frequency is irregular and nonlinear. The experimental results of Zhou et al. (2015) also verified similar phenomena. This is because all the droplets are almost stationary under the actions of sound waves of excessively high frequencies, whereas, the velocity variation of the droplets is close to the velocity oscillation of the fluid driven by sound waves at excessively low frequencies. In high-frequency cases, the relative motion between the droplets is marginal. In this study, an optimal sound frequency is considered, at which the difference in oscillatory motion of droplets of different sizes is maximal. In general, the acoustic agglomeration is considerably sensitive to the frequency of sound waves.

c. *SPL effect on the collision of two droplets*

Figure 8 shows the coefficient of the collision location under the action of sound waves of 50 Hz with different SPL for different combination of droplet sizes. The influence of the SPL on cloud droplets collision can be divided into three stages according to the curves in Fig. 8: 1) For a lower SPL, the sound field exerts negligible effect on the motion of both the cloud droplets, and the collision time undergoes negligible variation as compared with the case where sound wave is absent. 2) With

TABLE 2. Variation range of collision time and location for different droplet combinations under the action of sound waves of 123.4 dB.

Sound frequency (Hz)	20	50	60	80	100	200	400
Min coef of collision time (%)	−10.81	−16.51	−9.51	−12.86	−9.13	−4.72	−2.89
Max coef of collision time (%)	49.06	12.14	16.98	15.09	6.92	5.02	3.14
Max coef of collision location (%)	156.82	58.66	52.54	39.12	22.18	14.69	7.99

the increase in the SPL, the sound wave first causes a large vibration of the small droplets, and the increase in its displacement is larger than that of the large droplets. Thereby, the collision time increases. 3) When the SPL is adequately high, the large cloud droplets accelerate to catch up with the small cloud droplets, and the collision time decreases rapidly. These three stages behave differently for different droplet size combinations. When the droplet size is small with negligible difference, the second stage is not apparent. This is because the responses of the two droplet sizes to the SPL are almost identical, as shown in Fig. 8a. When d2 is large, only a displacement increment in small cloud droplets is caused within the given SPL range. The sound wave cannot significantly influence large droplets. Therefore, the third stage is not observed, such as in the case of d2 = 100 μm. When the cloud droplets are large and substantially different from each other, the promotion effect of the sound wave on d1 is not significant relative to the falling process of d2. Only an attenuation of the collision time owing to the accelerated motion of the large-sized cloud droplet can be observed, such as in the case where d1 = 10 and d2 = 50 μm (Fig. 8c). Only when the particle size is large and the difference between the droplet sizes is within a certain range, the three trends can be observed clearly.

Figures 8b, 8d, 8f, 8h, and 8j show the coefficients of the collision location under the action of sound waves of 50 Hz and different SPLs for different combinations of droplet sizes. The

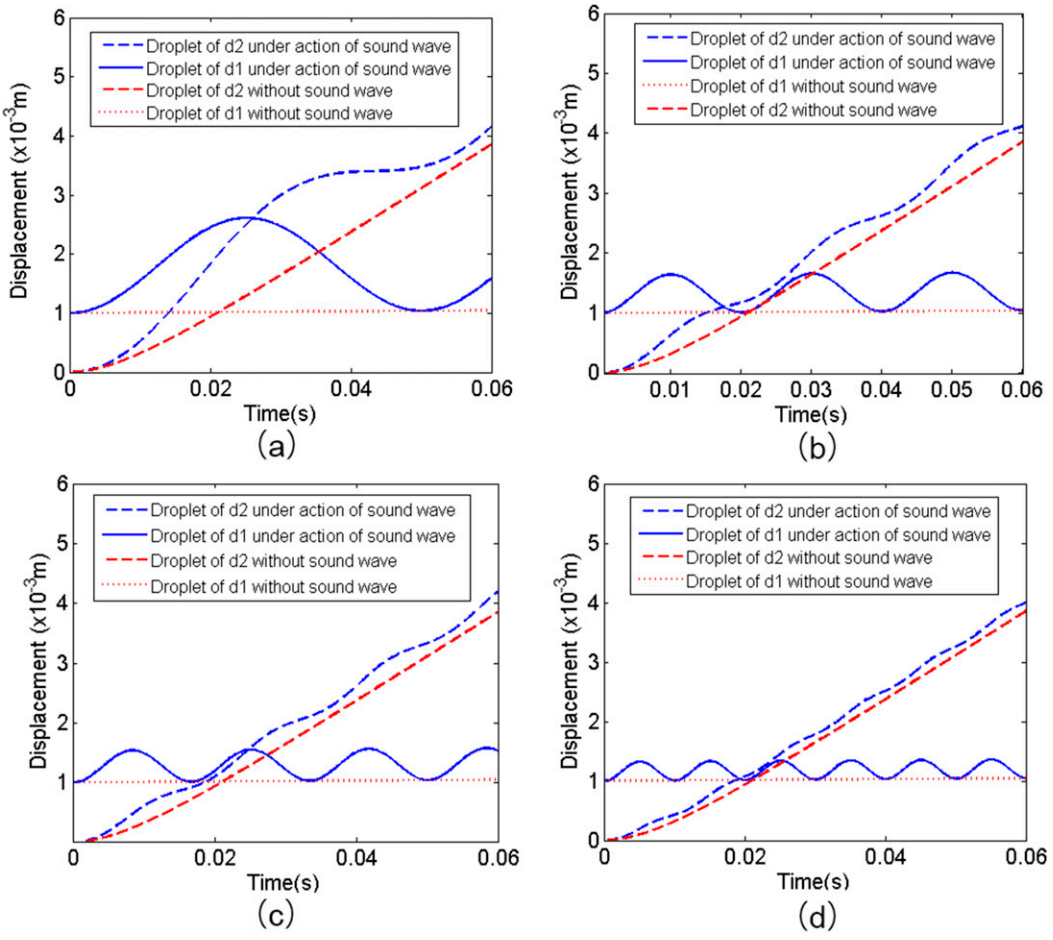

FIG. 7. Displacement variation of droplets with time considering the location of droplet without sound waves as the reference, under the action of sound waves of 123.4 dB and (a) 20, (b) 50, (c) 60, and (d) 100 Hz. Here, the droplet sizes d1 = 5 μm and d2 = 50 μm.

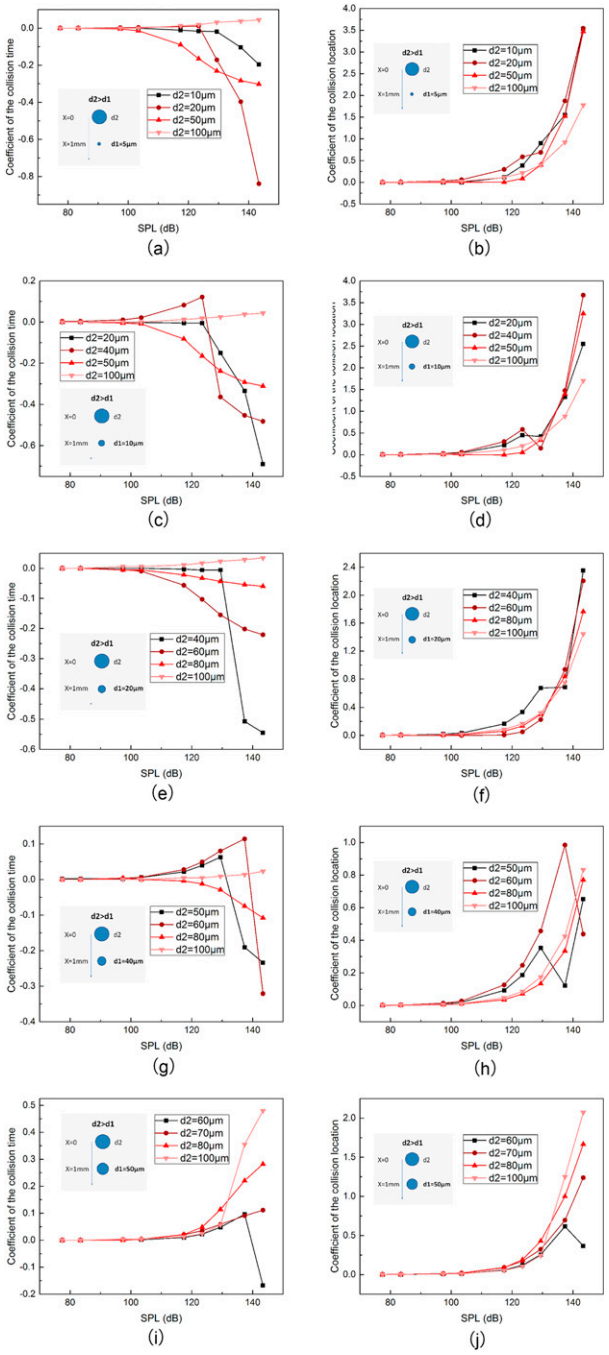

FIG. 8. Variation in coefficient of collision (left) time and (right) location with SPL for different droplet size combinations, under the action of sound waves of 50 Hz.

η_s varies significantly as compared with η_t, with a maximal value of 3.7. Unlike the influence of sound frequency, the variation trend of collision time and location at different SPLs is not synchronous. In general, a higher SPL corresponds to a shorter time required for collision as well as a larger cumulative displacement of the collision location. A significant reduction in the collision time and a significant increase in the collision displacement for the droplets can be achieved simultaneously under the action of sound waves of high SPL.

Table 3 presents the variation range of the collision time and location under the action of sound waves of different SPLs for different droplet size combinations. It is evident that both the variation amplitude of the collision time and the increment in the cumulative displacement increases with the increase in the SPL. Therefore, a sound wave significantly influences the collision between small droplets only when the SPL attains a threshold. Liu et al. (2009) reported that acoustic agglomeration is negligible when the SPL is below 132 dB for coal-fired fly ash particles of size less than 10 μm; an SPL above 140 dB is required to achieve effective agglomeration. Table 3 also indicates that when SPL = 143.4 dB, the coefficient of the collision time ranges from −84% to 48%, and the displacement increases by a factor of 3.7.

Figure 9 shows the positional variations for two droplets with d1 = 40 and d2 = 50 μm, without and with sound waves of 50 Hz. It indicates that the variation in SPL causes the intensity difference of the displacement oscillation and thereby, the difference in collision time and location. For a marginal SPL, the energy of the sound wave is too small to cause apparent fluctuations of the droplets. As the SPL increases, the oscillation characteristics of the droplets become more pronounced. Moreover, Fig. 9 shows that the violent fluctuation of the displacement results in a gradual advancement of the intersection points of the two blue lines. That is, the time required for the collision shortens, and the displacement of the collision location increases for all the SPLs in Fig. 9.

In the absence of sound waves, the collision of large cloud droplets under the action of gravity, with other small cloud droplets encountered along its falling path is considered to be an important mechanism for the growth of cloud droplets into raindrops (Saffman and Turner 1956).

In this paper, the criterion for the significant impact of sound waves on cloud droplet collision is defined as 1) the difference between the maximum collision time coefficient and the minimum collision time coefficient is greater than 10%, and 2) the maximum collision displacement coefficient is greater than 20%, as shown here:

$$\begin{cases} (\eta_t^{\max} - \eta_t^{\min}) \geq 10\% \\ \eta_s^{\max} \geq 20\% \end{cases}. \tag{16}$$

It can be concluded from Tables 2 and 3 that when the acoustic frequency is less than 100 Hz (at 123.4 dB) or the sound pressure level is greater than 117.4 dB (at 50 Hz), the sound wave has a significant impact on the collision of the two cloud droplets.

5. Discussion and conclusions

The motion of cloud droplets under the actions of the traveling-wave sound field and the gravity field is theoretically analyzed and numerically solved in this study. The investigations included the force analysis of an individual droplet and the relative motion analysis of a pair of droplets. The results indicate the following:

TABLE 3. Variation range of collision time and location for different droplet combinations under the action of sound waves of 50 Hz.

SPL (dB)	103.4	117.4	123.4	137.4	143.4
Min coef of collision time (%)	−1.42	−8.96	−16.51	−50.72	−83.89
Max coef of collision time (%)	2.14	8.21	12.14	35.48	47.98
Max coef of collision location (%)	6.04	30.19	58.66	187.38	367.20

1) The falling velocity of cloud droplets in a sound field reflects the characteristics of periodic oscillation. The equilibrium velocity is equal to the free settling velocity, which is related only to the droplet size. Smaller cloud droplets display apparent fluctuations in the velocity and displacement in the sound field. With growth in the droplet size, the motion state approaches the case without sound waves.
2) The frequency and SPL of sound waves mainly affect the period and amplitude of the variation in droplet velocity. With an increase in the sound frequency, the amplitude of droplet velocity decreases. The oscillation frequency of droplet velocity is in accordance with that of the sound wave. The velocity amplitude of the cloud droplet exhibits a linear correlation with that of the fluid. There exists a size threshold of the droplet being easily driven by sound waves of 50 Hz and 123.4 dB, which is equal to 40 μm; that is, droplets smaller than 40 μm can be easily driven by this sound, whereas those larger than 40 μm can be hardly driven by the same sound.
3) A sound wave significantly influences the collision process between two cloud droplets when the sound frequency is low and SPL is high. A numerical solution of the collision process of two falling droplets reveals that the variation in the period of droplet displacement and that in the

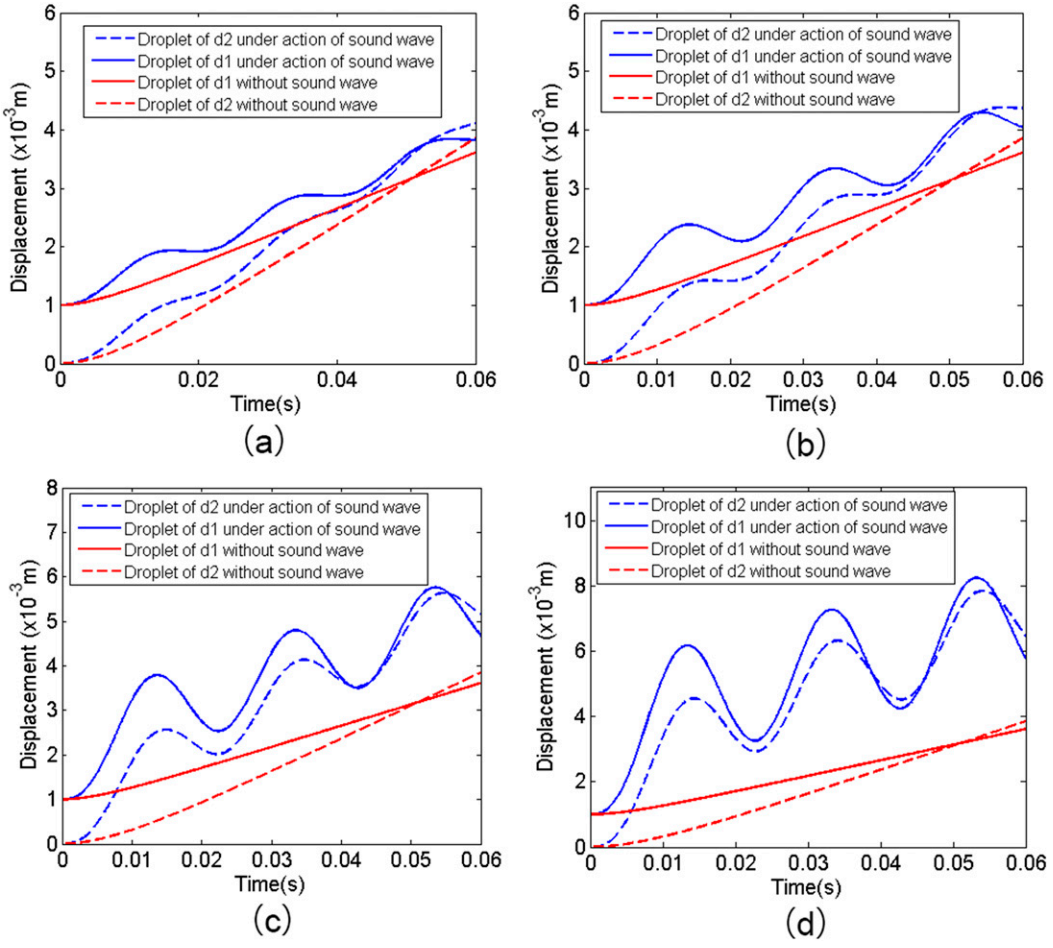

FIG. 9. Displacement variation of droplets with time considering the location of droplet d1 without sound waves as the reference, under the action of sound waves of 50 Hz and (a) 123.4, (b) 129.4, (c) 137.4, and (d) 143.4 dB. Here, the droplet size d1 = 40 μm and d2 = 50 μm.

amplitude of droplet fluctuation caused by the sound wave results in an unstable variation in the collision time. As the sound frequency increases, the influence of the sound waves reduces. Furthermore, as the SPL increases, the collision time and location varies more drastically. The frequency range of sound waves that significantly affect collision is concentrated in the low-frequency region. The calculation reveals that under the action of sound waves of SPL 143.4 dB and frequency 50 Hz, the collision time varies from −84% to 48%, and the displacement of the collision location increases by a factor of 3.7. Under the action of certain sound waves, the collision process of cloud droplets expands on both the spatial and temporal scales, making much more chaos of the system. This may increases the probability of cloud droplet collision. This study found when the acoustic frequency is less than 100 Hz (at 123.4 dB) or the SPL is greater than 117.4 dB (at 50 Hz), the sound wave has a significant impact on the collision of cloud droplets.

This study verifies that the presence of sound waves induces oscillatory motion of individual cloud droplets and aggravates the degree of disorderliness of motion for polydisperse cloud droplet groups. The displacement of a droplet increases noticeably under the action of sound waves of a certain SPL and frequency. Yang et al. (2019) verified that sound waves could also accelerate the movement of the atmospheric aerosol, which is conducive to the condensation of cloud droplets. Kumar and Suzuki (2019) considered that destroying the stability of clouds is conducive to the formation of rainfall. Therefore, it can be inferred that sound waves increase the probability of collision between cloud droplets by causing turbulent-like motion of the cloud droplets, thereby promoting the collision and growth of raindrops. Note that the direction of a sound wave was assumed to be vertical in this paper, and the effect of horizontal acoustic waves was not discussed. Droplets may be more significantly affected by sound waves in horizontal direction vertically coupled with the effect of gravitational sedimentation. However, further studies are needed to confirm it.

The collisional efficiency of cloud droplets is a traditional concept with clear physical meaning and mathematical description in the classical gravitational collision model (Lamb and Verlinde 2011). The traditional cloud droplet gravitational collision model can explain the mechanism of the increase of the collision probability when the acoustic wave oscillation is perpendicular to the falling cloud droplet. We also recognize that the classical model has not yet been used to explain the promoting effect of vertical acoustic wave oscillation. However, in real fog conditions, only a few cloud droplets have acoustic oscillation in the completely vertical direction, and most of them have horizontal acoustic oscillation component. Therefore, we think that the classical gravitational collision model of cloud droplets is consistent with and complementary to the mechanism of acoustic wave promoting the growth of raindrop collision. On the other hand, through the experimental study, we also proved that the growth and evolution of the suspended cloud droplets can be influenced by the application of acoustic waves from both horizontal (Cao et al. 2021) and vertical (Qiu et al. 2021) directions. Further study is necessary to improve the understanding of the promoting mechanism of vertical acoustic wave on droplet collision. This study deepens the understanding of the interaction between sound waves and cloud droplets and provides a theoretical analysis basis for the application of strong sound waves to technical issues such as dehumidification, fog removal, and rainfall enhancement.

Acknowledgments. This research was supported by the Integration Program of the Major Research Plan of the National Natural Science Foundation of China (91847302), National Natural Science Foundation of China (51879137, 51979276).

Data availability statement. The data and code used during the study are available from the corresponding author by request.

REFERENCES

Akimov, I. V., 2004: Precipitation calculation method based on parameterization of distribution function evolution and its performance in global spectral atmospheric model. *J. Hydrol.*, **288**, 105–120, https://doi.org/10.1016/j.jhydrol.2003.11.012.

Amiri, M., A. Sadighzadeh, and C. Falamaki, 2016: Experimental parametric study of frequency and sound pressure level on the acoustic coagulation and precipitation of $PM_{2.5}$ aerosols. *Aerosol Air Qual. Res.*, **16**, 3012–3025, https://doi.org/10.4209/aaqr.2015.12.0683.

Basset, B. A., 1888: *A Treatise on Hydrodynamics*. George Bell and Sons, 372 pp.

Bhartend, 1969: Audio frequency pressure variations from lightning discharges. *J. Atmos. Terr. Phys.*, **31**, 743–747.

Bodhika, J. A. P., W. G. D. Dharmarathna, M. Fernando, and V. Cooray, 2018: Characteristics of thunder pertinent to tropical lightning. *34th Int. Conf. on Lightning Protection (ICLP)*, Rzeszow, Poland, Institute of Electrical and Electronics Engineers, 287–292, https://doi.org/10.1109/ICLP.2018.8503455.

Cao H, F.-F. Li, X. Zhao, Z.-L. Liu, G.-Q. Wang, and J. Qiu, 2021: Micro-droplet deposition and growth on a glass slide driven by acoustic agglomeration. *Exp. Fluids*, **62**, 127, https://doi.org/10.1007/s00348-021-03215-6.

Cleckler, J., S. Elghobashi, and F. Liu, 2012: On the motion of inertial particles by sound waves. *Phys. Fluids*, **24**, 24, https://doi.org/10.1063/1.3696243.

Dong, S. Z., B. Lipkens, and T. M. Cameron, 2006: The effects of orthokinetic collision, acoustic wake, and gravity on acoustic agglomeration of polydisperse aerosols. *J. Aerosol Sci.*, **37**, 540–553, https://doi.org/10.1016/j.jaerosci.2005.05.008.

Fan, F. X., M. J. Zhang, and C. N. Kim, 2013: Numerical simulation of interaction between two $PM_{2.5}$ particles under acoustic travelling wave conditions. *AIP Conf. Proc.*, **1542**, 855–858, https://doi.org/10.1063/1.4812066.

Finlay, W.H., 2001: *Motion of a Single Aerosol Particle in a Fluid*. Academic Press, 302 pp.

Galechyan, G. A., 2005: On acoustic stimulation of atmospheric precipitation. *Tech. Phys.*, **50**, 1191–1194, https://doi.org/10.1134/1.2051461.

Gallego-Juárez, J. A., and Coauthors, 1999: Application of acoustic agglomeration to reduce fine particle emissions from coal

combustion plants. *Environ. Sci. Technol.*, **33**, 3843–3849, https://doi.org/10.1021/es990002n.

Grabowski, W. W., and L. P. Wang, 2013: Growth of cloud droplets in a turbulent environment. *Annu. Rev. Fluid Mech.*, **45**, 293–324, https://doi.org/10.1146/annurev-fluid-011212-140750.

Hassan, S., and M. Kawaji, 2008: The effects of vibrations on particle motion in a viscous fluid cell. *J. Appl. Mech.*, **75**, 031012, https://doi.org/10.1115/1.2839658.

Hoffmann, T. L., 2000: Environmental implications of acoustic aerosol agglomeration. *Ultrasonics*, **38**, 353–357, https://doi.org/10.1016/S0041-624X(99)00184-5.

Hou, S., J. Wu, and B. Xi, 2002: Experimental study on the effect of low-frequency acoustic wave on water mist dissipation (in Chinese). *Hydrodyn. Exp. Meas.*, **16** (4), 52–56, 63.

Kačianauskas, R., V. Rimsa, A. Kaceniauskas, A. Maknickas, D. Vainorius, and R. Pacevic, 2018: Comparative DEM-CFD study of binary interaction and acoustic agglomeration of aerosol microparticles at low frequencies. *Chem. Eng. Res. Des.*, **136**, 548–563, https://doi.org/10.1016/j.cherd.2018.06.006.

Kim, I., S. Elghobashi, and W. A. Sirignano, 1998: On the equation for spherical-particle motion: Effect of Reynolds and acceleration numbers. *J. Fluid Mech.*, **367**, 221–253, https://doi.org/10.1017/S0022112098001657.

Knoop, C., and U. Fritsching, 2014: Dynamic forces on agglomerated particles caused by high-intensity ultrasound. *Ultrasonics*, **54**, 763–769, https://doi.org/10.1016/j.ultras.2013.09.022.

Kumar, K. N., and K. Suzuki, 2019: Assessment of seasonal cloud properties in the United Arab Emirates and adjoining regions from geostationary satellite data. *Remote Sens. Environ.*, **228**, 90–104, https://doi.org/10.1016/j.rse.2019.04.024.

Lamb, D., and J. Verlinde, 2011: *Physics and Chemistry of Clouds*. Cambridge University Press, 584 pp.

Li, F., Y. Jia, G. Wang, and J. Qiu, 2020: Mechanism of cloud droplet motion under sound wave actions. *J. Atmos. Oceanic Technol.*, **37**, 1539–1550, https://doi.org/10.1175/JTECH-D-19-0210.1.

Liu, C., Z. Tian, Y. Zhao, and X. Zeng, 2020: Review and prospect of fog elimination technology based on acoustic condensation. *IOP Conf. Ser. Earth Environ. Sci.*, **514**, 032011, https://doi.org/10.1088/1755-1315/514/3/032011.

Liu, J. Z., G. X. Zhang, J. H. Zhou, J. Wang, W. D. Zhao, and K. F. Cen, 2009: Experimental study of acoustic agglomeration of coal-fired fly ash particles at low frequencies. *Powder Technol.*, **193**, 20–25, https://doi.org/10.1016/j.powtec.2009.02.002.

Markauskas, D., R. Kačianauskas, and A. Maknickas, 2015: Numerical particle-based analysis of the effects responsible for acoustic particle agglomeration. *Adv. Powder Technol.*, **26**, 698–704, https://doi.org/10.1016/j.apt.2014.12.008.

Maxey, M. R., and J. J. Riley, 1983: Equation of motion for a small rigid sphere in a nonuniform flow. *Phys. Fluids*, **26**, 883–889, https://doi.org/10.1063/1.864230.

McDonald, J. E., 1958: The physics of cloud modification. *Adv. Geophys.*, **5**, 223–303, https://doi.org/10.1016/S0065-2687(08)60079-5.

Mednikov, E. P., and C. V. Larrick, 1965: Acoustic coagulation and precipitation of aerosols. *Appl. Mech. Mater.*, **34**, 1087–1103.

Mei, R. W., and R. J. Adrian, 1992: Flow past a sphere with an oscillation in the free-stream velocity and unsteady drag at finite Reynolds number. *J. Fluid Mech.*, **237**, 323–341, https://doi.org/10.1017/S0022112092003434.

——, C. J. Lawrence, and R. J. Adrian, 1991: Unsteady drag on a sphere at finite Reynolds number with small fluctuations in the free-stream velocity. *J. Fluid Mech.*, **233**, 613–631, https://doi.org/10.1017/S0022112091000629.

Oseen, C. W., 1927: Hydrodynamik. *Scientia*, **22**, 343.

Otto, E., and H. Fissan, 1999: Brownian coagulation of submicron particles. *Adv. Powder Technol.*, **10** (1), 1–20, https://doi.org/10.1016/S0921-8831(08)60453-7.

Qiu, J., L. J. Tang, L. Cheng, G. Q. Wang, and F. F. Li, 2021: Interaction between strong sound waves and cloud droplets: Cloud chamber experiment. *Appl. Acoust.*, **176**, 107891, https://doi.org/10.1016/j.apacoust.2020.107891.

Saffman, P. G., and J. S. Turner, 1956: On the collision of drops in turbulent clouds. *J. Fluid Mech.*, **1**, 16–30, https://doi.org/10.1017/S0022112056000020.

Seinfeld, J. H., and S. N. Pandis, 1998: *Atmospheric Chemistry and Physics: From Air Pollution to Climate Change*. John Wiley and Sons, 1120 pp.

Sepehrirahnama, S., K. M. Lim, and F. S. Chau, 2015: Numerical analysis of the acoustic radiation force and acoustic streaming around a sphere in an acoustic standing wave. *Phys. Procedia*, **70**, 80–84, https://doi.org/10.1016/j.phpro.2015.08.047.

Shaw, D. T., and K. W. Tu, 1979: Acoustic particle agglomeration due to hydrodynamic interaction between monodisperse aerosols. *J. Aerosol Sci.*, **10**, 317–328, https://doi.org/10.1016/0021-8502(79)90047-8.

Sheng, C. D., and X. L. Shen, 2006: Modelling of acoustic agglomeration processes using the direct simulation Monte Carlo method. *J. Aerosol Sci.*, **37**, 16–36, https://doi.org/10.1016/j.jaerosci.2005.03.004.

Sheng, P.-X., J.-T. Mao, J.-G. Li, A.-S. Zhang, J.-G. Sang, and N.-X. Pan, 2003: *Atmospheric Physics*. Peking University Press, 375 pp.

Sujith, R. I., G. A. Waldherr, J. I. Jagoda, and B. T. Zinn, 1997: An experimental investigation of the behavior of droplets in axial acoustic fields. *J. Vib. Acoust.*, **119**, 285–292, https://doi.org/10.1115/1.2889722.

——, ——, ——, and ——, 1999: A theoretical investigation of the behavior of droplets in axial acoustic fields. *J. Vib. Acoust.*, **121**, 286–294, https://doi.org/10.1115/1.2893978.

Talty, J. T., 1998: Physics of sound. *Industrial Hygiene Engineering*, 2nd ed. William Andrew Publishing, 372–389.

Tulaikova, T., 2015: Acoustical method and device for precipitation enhancement inside natural clouds. *Sci. Discovery*, **3**, 18–25, https://doi.org/10.11648/j.sd.s.2015030201.13.

Wallace, J. M., and P. V. Hobbs, 2006: *Atmospheric Science: An Introductory Survey*. 2nd ed. Elsevier Science, 483 pp.

Wei, J., Y. Li, D. Chen, A. S. Nwankwegu, C. Tang, M. Bu, and S. Zhang, 2020: The influence of ship wave on turbulent structures and sediment exchange in large shallow Lake Taihu, China. *J. Hydrol.*, **586**, 124853, https://doi.org/10.1016/j.jhydrol.2020.124853.

——, J. Qiu, T. Li, Y. Huang, Z. Qiao, J. Cao, D. Zhong, and G. Wang, 2021: Cloud and precipitation interference by strong low-frequency sound wave. *Sci. China Technol. Sci.*, **64**, 261–272, https://doi.org/10.1007/s11431-019-1564-9.

Wieprecht, W., K. Acker, S. Mertes, J. Collett, W. Jaeschke, E. Bruggemann, D. Moller, and H. Herrmann, 2005: Cloud physics and cloud water sampler comparison during FEBUKO. *Atmos. Environ.*, **39**, 4267–4277, https://doi.org/10.1016/j.atmosenv.2005.02.012.

Yang, Y., and Coauthors, 2019: Toward understanding the process-level impacts of aerosols on microphysical properties of shallow cumulus cloud using aircraft observations. *Atmos. Res.*, **221**, 27–33, https://doi.org/10.1016/j.atmosres.2019.01.027.

Yuhua, O. Y., and Y. Ping, 2012: Audible thunder characteristic and the relation between peak frequency and lightning parameters. *J. Earth Syst. Sci.*, **121**, 211–220, https://doi.org/10.1007/s12040-012-0147-0.

Zeng, C., W. Deng, J. Fan, and Y. D. Zhang, 2020: Effect of flow profiles on the flow subjected to oscillation forcing: An example of droplet mobilization in constricted tubes. *J. Hydrol.*, **583**, 124295, https://doi.org/10.1016/j.jhydrol.2019.124295.

Zhang, B., M. Zhu, C. Wang, and X. Guan, 2012: Analysis of cloud droplets growth and phase transition radiation process. *Energy Procedia*, **16**, 1003–1008, https://doi.org/10.1016/j.egypro.2012.01.160.

Zhang, G. X., Z. F. Ma, J. Shen, K. Zhang, J. Q. Wang, and Z. H. Chi, 2020: Experimental study on eliminating fire smokes using acoustic agglomeration technology. *J. Hazard. Mater.*, **382**, 121089, https://doi.org/10.1016/j.jhazmat.2019.121089.

Zhang, X., C. Gan, and R. Wei, 1963: Preliminary experimental study on the effect of sound wave on water mist dissipation (in Chinese). *J. Nanjing Univ.*, **3**, 21–27.

Zheng, J. X., Y. K. Li, Z. Q. Wan, W. P. Hong, and L. Wang, 2019: Modification of the agglomeration kernel and simulation of the flow pattern in acoustic field with fine particles. *Powder Technol.*, **356**, 930–940, https://doi.org/10.1016/j.powtec.2019.09.022.

Zhou, D., Z. Luo, M. Fang, H. Xu, J. Jiang, Y. Ning, and Z. Shi, 2015: Preliminary experimental study of acoustic agglomeration of coal-fired fine particles. *Procedia Eng.*, **102**, 1261–1270, https://doi.org/10.1016/j.proeng.2015.01.256.

Zu, K., Y. Yao, M. Cai, F. Zhao, and D. L. Cheng, 2017: Modeling and experimental study on acoustic agglomeration for dust particle removal. *J. Aerosol Sci.*, **114**, 62–76, https://doi.org/10.1016/j.jaerosci.2017.09.001.